POLITECNICO DI TORINO
Repository ISTITUZIONALE

Combining multiple Large Volume Metrology systems: Competitive versus cooperative data fusion

(Article begins on next page)

28 April 2024

Combining multiple Large Volume Metrology systems: competitive versus cooperative data fusion

Fiorenzo Franceschini[1], Maurizio Galetto[2], Domenico Maisano[3] and Luca Mastrogiacomo[4]

[1] fiorenzo.franceschini@polito.it   [2] maurizio.galetto@polito.it   [3] domenico.maisano@polito.it
[4] luca.mastrogiacomo@polito.it

Politecnico di Torino, DIGEP (Department of Management and Production Engineering),
Corso Duca degli Abruzzi 24, 10129, Torino (Italy)

Abstract

Large Volume Metrology (LVM) tasks can require the concurrent use of several measuring systems. These systems generally consist of set of sensors measuring the distances and/or angles with respect to a point of interest so as to determine its 3D position. When combining different measuring systems, characterized by sensors of different nature, competitive or cooperative methods can be adopted for fusing data. Competitive methods, which are by far the most diffused in LVM, basically perform a weighted mean of the 3D positions determined by the individual measuring systems. On the other hand, for cooperative methods, distance and/or angular measurements by sensors of different systems are combined together in order to determine a unique 3D position of the point of interest.

This paper proposes a novel cooperative approach which takes account of the measurement uncertainty in distance and angular measurements of sensors of different nature. The proposed approach is compared with classical competitive approaches from the viewpoint of the metrological performance. The main advantages of the cooperative approach, with respect to the competitive one, are: (i) it is the only option when the individual LVM systems are not able to provide autonomous position measurements (e.g., laser interferometers or single cameras), (ii) it is the only option when only some of the sensors of autonomous systems work correctly (for instance, a laser tracker in which only distance – not angular – measurements are performed), (iii) when using systems with redundant sensors (i.e. photogrammetric systems with a large number of distributed cameras), point localization tends to be better than that using the competitive fusion approach.

Keywords: Cooperative fusion, Competitive fusion, Large volume metrology, Large Scale Dimensional Metrology, Hybrid localization.

1. Introduction and literature review

Sensor fusion can be defined as the combination of sensory data from different sources, so that the resulting information is somehow better than the information deriving from the single sources taken separately (Crowley and Demazeau, 1993; Haghighat et al., 2011). The term "better" can assume different meanings depending to the context of interest: it can mean more accurate, more complete, more reliable, etc. In their survey, Weckenmann et al. (2009) define the concept of *multisensor data fusion* in dimensional metrology as "the process of combining data from several information sources (sensors) into a common representational format in order that the metrological evaluation can benefit from all available sensor information and data".

An individual dimensional metrology system is basically able to collect and process several input

1

data, deriving from a set of sensors, so as to provide an output, generally the dimensional coordinates of the point of interest (see figure 1). It generally consists of:

- A set of sensors, i.e. devices able to measure primary geometric quantities, such as distances and angles.
- A Data Processing Unit (DPU), which processes sensory data in order to provide an estimation of the 3D position of the point of interest.
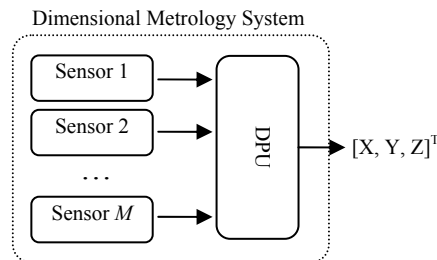
Figure 1. Schematic representation of a generic dimensional metrology system. The Data Processing Unit (DPU) gathers and processes sensory data to output the 3D coordinates of the point of interest, i.e. [X, Y Z]^T.

Typical industrial applications are the reconstruction of curves/surfaces for dimensional verification and/or the assembly of large-sized mechanical components.

According to the sensors layout, dimensional metrology systems can be classified as (i) *centralized*, if sensors are grouped into a unique stand-alone unit, or (ii) *distributed*, if sensors are spread around the measuring volume (Xiong and Svensson, 2002; Maisano et al., 2009; Maisano and Mastrogiacomo, 2015).

Large Volume Metrology (LVM) tasks often involve the concurrent use of multiple dimensional metrology systems (for instance, two or more laser trackers, or scanners, combined with a distributed photogrammetric system, etc.) (Calkins and Salerno, 2000; Weckenmann et al., 2009; Franceschini et al., 2011; Galetto and Mastrogiacomo, 2013). This practice has several benefits including but not limited to: (i) overcoming the limitations of the individual system; (ii) improving measurement accuracy; (iii) taking advantage of the overall available instrumentation; (iv) reducing the risk of measurement errors.

The concurrent use of multiple systems requires the definition of suitable data fusion strategies. Two possible approaches can be adopted (Durrant-Whyte, 1988; Haghighat et al., 2011):

- *Competitive* fusion. Each system performs an independent measurement of the 3D coordinates of the point of interest and these position measurements are fused into a single one (Boudjemaa and Forbes, 2004). This fusion approach is defined as competitive, since each system "compete" for the definition of the fusion result. For example, this principle is implemented in the SpatialAnalyser®, probably the most diffused software for LVM applications (New River Kinematics, 2015). The goal of competitive fusion is to improve

the measurement accuracy while reducing the risk of measurement errors (Boudjemaa and Forbes, 2004).

- *Cooperative* Fusion. Data provided by two or more independent (non homogeneous) sensors, even from different measuring systems are processed in order to achieve information that otherwise could not be obtained from individual sensors (Boudjemaa and Forbes, 2004). According to this logic, the different sensors share their local measurements and "cooperate" for determining a unique position measurement of the point of interest. For example, data from (i) two sensors of a system performing angular measurements, and (ii) one sensor of another system performing distance measurements can be combined for determining the 3D coordinates of the point of interest.

Compared to the competitive data-fusion approach, the cooperative one is more difficult to implement, as it requires that the individual measurement systems are able to return "intermediate" data, such as distance and angular measurements by the relevant sensors. However it will be shown that a cooperative fusion approach could potentially make a more efficient use of the information available, resulting in improved metrological performance. Also, it is the only option when dealing with sensors that, taken separately, are not able to perform independent localizations of the point of interest (for instance a laser interferometer combined with a single photogrammetric camera) (Galetto et al., 2015).

While the scientific literature encompasses several descriptions of the competitive approaches (Boudjemaa and Forbes, 2004), the cooperative ones are almost totally ignored or confined to specific measurement applications (Beckerman and Sweeney, 1994; Ho and Pong, 1996; Labayrade et al., 2005; Lamallem et al., 2009; Wen et al., 2010; Budzan, 2014).

This paper proposes a novel cooperative approach which takes account of the measurement uncertainty in distance and angular measurements of sensors of different nature. The proposed approach will be compared with classical competitive approaches from the viewpoint of the metrological performance.

The remainder of the paper is structured as follows. Sect. 2 introduces the problem of data-fusion in dimensional metrology throughout an introductory example, while the problem is formalized in Sect. 3. Sect. 4 discusses the classical competitive approach, also proposing a generalized cooperative approach. Sect. 5 reports a benchmarking between the proposed approach and a classical competitive approach, based on real and simulated experiments. The concluding section summarizes the original contributions of the paper, focusing on the benefits, limitations and possible future developments.

2. Introductory example

Before providing a comprehensive description of the competitive and cooperative approaches, we present an introductory example to illustrate the data-fusion problem. Let us consider a measurement volume covered by two LVM systems (see Figure 2):

- A photogrammetric system (PS), which is able to determine the position of a target in contact with the object to be measured. Precisely, this system includes several cameras distributed around the measurement volume, able to determine the 2-D position of the target within the local image and determining the angles subtended by the target with respect to the camera's focal point (Franceschini et al., 2011). The 3-D coordinates of the target are then determined, combining the local measurements by the individual cameras (Luhmann et al., 2006; Franceschini et al., 2011).

- A Laser Tracker (LT), which is able to measure the 3-D coordinates of a point by tracking a laser beam from the instrument to a retro-reflective target, in contact with the object to be measured. The position of the retro-reflective target is calculated using the distance ($\hat{d}_{LT}$) and the angular ($\hat{\theta}_{LT}$ and $\hat{\varphi}_{LT}$) measurements subtended by the target.
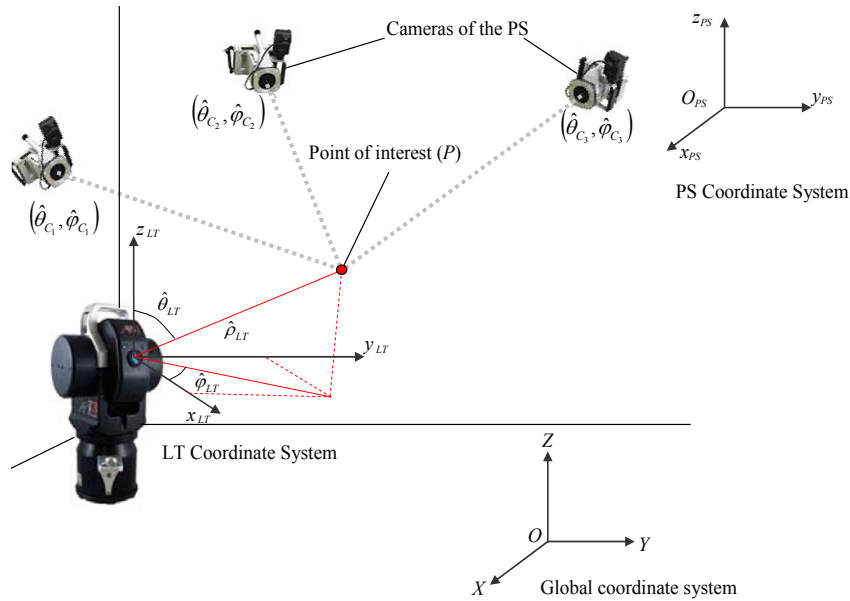
Figure 2. Example of concurrent measurement by two LVM systems: a laser tracker (LT) and a photogrammetric system (PS).

In the layout proposed in Fig.2, the PS includes a set of 3 cameras. Each i-th camera performs azimuth ($\hat{\theta}_{C_i}$) and elevation ($\hat{\varphi}_{C_i}$) angular measurement with respect to the point of interest. Next, the position of P can be calculated combining the local measurements from the three cameras; in formal terms:

$$\hat{\mathbf{x}}_{P_{PS}} = \left[x_{P_{PS}}, y_{P_{PS}}, z_{P_{PS}}\right]^T = f_{PS}\left(\left(\hat{\theta}_{C_1}, \hat{\varphi}_{C_1}\right), \left(\hat{\theta}_{C_2}, \hat{\varphi}_{C_2}\right), \left(\hat{\theta}_{C_3}, \hat{\varphi}_{C_3}\right)\right), \tag{1}$$

where:

- $\hat{\mathbf{x}}_{P_{PS}}$ is the estimate of the position of P;

- $\hat{\theta}_{C_i}$ and $\hat{\varphi}_{C_i}$ are local angular measurements performed by each i-th camera;

- f_{PS} is a suitable function for turning local angular measurements into $\hat{\mathbf{x}}_{P_{PS}}$;

The proposed layout also includes a LT which is typically equipped with an absolute distance meter (ADM) and/or a laser interferometer (performing distance measurements ($\hat{\rho}_{LT}$)) and two angular encoders (performing angular measurements, i.e. azimuth ($\hat{\theta}_{LT}$) and elevation ($\hat{\varphi}_{LT}$) with respect to P). As for the PS, the LT is able to estimate the position of P using the available local measurements:

$$\hat{\mathbf{x}}_{P_{LT}} = \left[x_{P_{LT}}, y_{P_{LT}}, z_{P_{LT}}\right]^T = f_{LT}\left(\hat{\rho}_{LT}, \hat{\theta}_{LT}, \hat{\varphi}_{LT}\right). \tag{2}$$

being

- $\hat{\mathbf{x}}_{P_{LT}}$ is the estimate of the position of P;

- $\hat{\rho}_{LT}, \hat{\theta}_{LT}$ and $\hat{\varphi}_{LT}$ are local distance and angular measurements performed by the LT;

- f_{LT} is a suitable function for turning local measurements into $\hat{\mathbf{x}}_{P_{LT}}$;

Although the two systems are able to operate independently, their combined use could lead to the aforementioned advantages. So, how to take advantage of both the systems? What is the most appropriate strategy?

The most obvious and immediate approach would be that of averaging of the position estimates ($\hat{\mathbf{x}}_{P_{PS}}$ and $\hat{\mathbf{x}}_{P_{LT}}$) provided by the two systems. However, this is certainly not the most efficient approach since it neglects the metrological performance (i.e. the measurement uncertainty) of the individual systems and the fact that the estimate of one system can be significantly better than that of the other system. In typical competitive approaches, this problem can be overcome aggregating $\hat{\mathbf{x}}_{P_{PS}}$ and $\hat{\mathbf{x}}_{P_{LT}}$ by weighted average, where weights take account of measurement uncertainty of the single LVM system; in formal terms:

$$\hat{\mathbf{x}}_{P_{COMP}} = \left[x_{P_{COMP}}, y_{P_{COMP}}, z_{P_{COMP}}\right]^T = f_{COMP}\left(\hat{\mathbf{x}}_{P_{LT}}, \hat{\mathbf{x}}_{P_{PS}}\right), \tag{3}$$

where:

- $\hat{\mathbf{x}}_{P_{COMP}}$ is the estimate of the position of P;

- $\hat{\mathbf{x}}_{P_{LT}}$ and $\hat{\mathbf{x}}_{P_{PS}}$ are the estimates of the position of P respectively given by the LT and the PS;

- f_{COMP} is a suitable function for combining $\hat{\mathbf{x}}_{P_{LT}}$ and $\hat{\mathbf{x}}_{P_{PS}}$ into $\hat{\mathbf{x}}_{P_{COMP}}$, considering individual system uncertainty;

On the other hand, the cooperative fusion approach aims at estimating the position of P as a function of the local angular and/or distance measurements by the individual sensors of the two systems, also considering its metrological characteristics; in formal terms:

$$\hat{\mathbf{x}}_{P_{COOP}} = \left[x_{P_{COOP}}, y_{P_{COOP}}, z_{P_{COOP}} \right]^T = f_{COOP}\left(\left(\theta_{C_1}, \varphi_{C_1}\right), \left(\theta_{C_2}, \varphi_{C_2}\right), \left(\theta_{C_3}, \varphi_{C_3}\right), \rho_{LT}, \theta_{LT}, \varphi_{LT} \right), \quad (4)$$

being:

- $\hat{\mathbf{x}}_{P_{COOP}}$ is the estimate of the position of P;

- $\hat{\theta}_{C_i}$ and $\hat{\varphi}_{C_i}$ are local angular measurements performed by each i-th camera;

- $\hat{\rho}_{LT}, \hat{\theta}_{LT}$ and $\hat{\varphi}_{LT}$ are local distance and angular measurements performed by the LT;

- f_{COOP} is a suitable function for determining the position of P from local sensor measurements, taking account of sensor measurement uncertainty;

3. Problem description

The problem herein discussed is to define of the 3D position of a point, combining the measurements of a number of LVM systems. Precisely, there are N LVM systems $(D_1,…,D_N)$, distributed over the measurement volume, so that each system is able to "see" the point of interest $(P \equiv [X, Y, Z]^T)$. Each i-th system consists of M_i sensors. A centralized data processing unit (DPU) receives and processes local measurement data from the totality of the sensors of the N LVM systems. A schematic representation of the problem architecture is shown in Figure 3.

Each j-th sensor from the i-th LVM system has its own spatial position and orientation, and local coordinate system o_{ij}-$x_{ij}y_{ij}z_{ij}$. A general transformation between a local and the global coordinate system (O-XYZ) is given by:

$$\mathbf{X} = \mathbf{R}_{ij}\mathbf{x}_{ij} + \mathbf{X}_{\mathbf{0}_{ij}} \Rightarrow \begin{bmatrix} X \\ Y \\ Z \end{bmatrix} = \begin{bmatrix} r_{11_{ij}} & r_{12_{ij}} & r_{13_{ij}} \\ r_{21_{ij}} & r_{22_{ij}} & r_{23_{ij}} \\ r_{31_{ij}} & r_{32_{ij}} & r_{33_{ij}} \end{bmatrix} \begin{bmatrix} x_{ij} \\ y_{ij} \\ z_{ij} \end{bmatrix} + \begin{bmatrix} X_{0_{ij}} \\ Y_{0_{ij}} \\ Z_{0_{ij}} \end{bmatrix}. \quad (5)$$
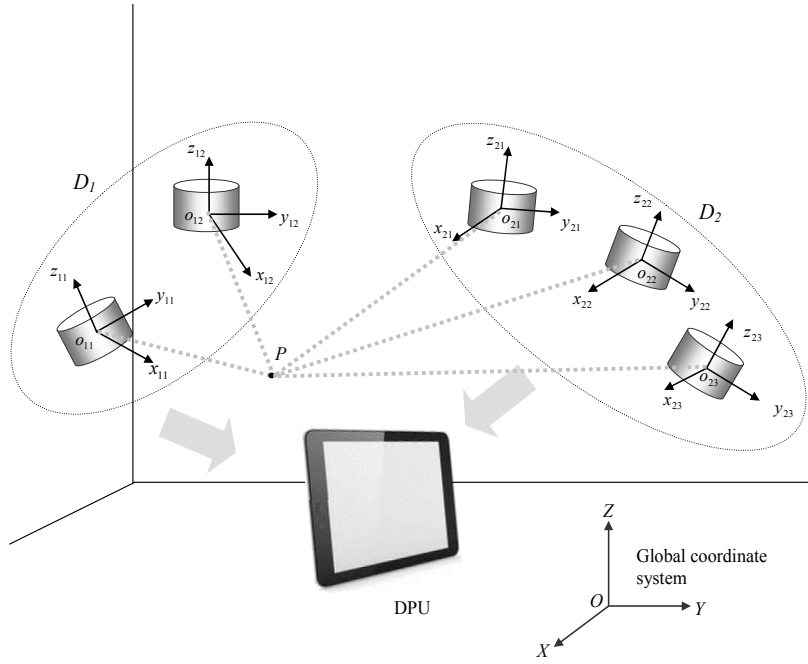
Figure 3. Schematic representation of the problem architecture. Two LVM systems (D_1 and D_2) are presented, respectively consisting of $M_1 = 2$ and $M_2 = 3$ sensors. P is the point to be measured. The data processing unit (DPU) gathers and processes the data obtained from the distributed sensors.

$\mathbf{X_{0_{ij}}} = \left[X_{0_{ij}}, Y_{0_{ij}}, Z_{0_{ij}} \right]^T$ are the coordinates of the origin of $o_{ij}\text{-}x_{ij}y_{ij}z_{ij}$ – i.e. the position of the j-th

sensor of the i-th LVM system – in the global coordinate system $O\text{-}XYZ$ and $\mathbf{x}_{ij} = \left[x_{ij}, y_{ij}, z_{ij} \right]^T$ are

the coordinates of P in the local coordinate system $o_{ij}\text{-}x_{ij}y_{ij}z_{ij}$. $\mathbf{R}_{ij}$ is a rotation matrix, which

elements are functions of three rotation angles (i.e. ω_{ij}, ϕ_{ij} and κ_{ij}, see Figure 4):
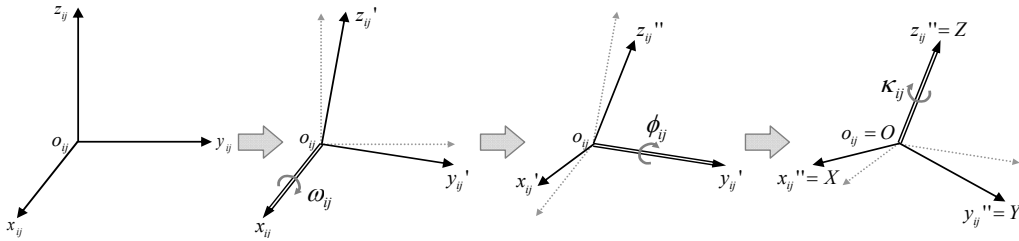
Figure 4. Rotation parameters regarding the transformation between a local coordinate system ($o_{ij}\text{-}x_{ij}y_{ij}z_{ij}$) and the global one ($OXYZ$).

$$\mathbf{R}_{ij} = \begin{bmatrix} \cos\phi_{ij}\cos\kappa_{ij} & -\cos\phi_{ij}\sin\kappa_{ij} & \sin\phi_{ij} \\ \cos\omega_{ij}\sin\kappa_{ij} + \sin\omega_{ij}\sin\phi_{ij}\cos\kappa_{ij} & \cos\omega_{ij}\cos\kappa_{ij} - \sin\omega_{ij}\sin\phi_{ij}\sin\kappa_{ij} & -\sin\omega_{ij}\cos\phi_{ij} \\ \sin\omega_{ij}\sin\kappa_{ij} - \cos\omega_{ij}\sin\phi_{ij}\cos\kappa_{ij} & \sin\omega_{ij}\cos\kappa_{ij} + \cos\omega_{ij}\sin\phi_{ij}\sin\kappa_{ij} & \cos\omega_{ij}\cos\phi_{ij} \end{bmatrix}, \quad (6)$$

where:

ω_{ij} represents a counterclockwise rotation around the x_{ij} axis;

ϕ_{ij} represents a counterclockwise rotation around the new y_{ij} axis (i.e., y_{ij}'), which was rotated by

ω_{ij};

κ_{ij} represents a counterclockwise rotation around the new z_{ij} axis (i.e., z_{ij}''), which was rotated by ω_{ij} and then ϕ_{ij}.

The (six) location/orientation parameters related to the j-th sensor in the i-th LVM system (i.e., $X_{0_{ij}}, Y_{0_{ij}}, Z_{0_{ij}}$, ω_{ij}, ϕ_{ij}, κ_{ij}) are considered as known parameters, since they are measured in an initial calibration process.

We remark that each i-th LVM system (D_i) is able to estimate the position of P autonomously. Let $\hat{\mathbf{X}}_{P_i} = \left[X_{P_i}, Y_{P_i}, Z_{P_i} \right]^T$ be the measurement of point P by D_i, expressed in the global coordinate system $O\text{-}XYZ$ through Eq. (5). The accuracy of D_i in measuring the coordinates of P can be quantified by defining the covariance matrix $\Sigma_{\hat{\mathbf{X}}_{P_i}}$.

Let $\mathbf{S}_{ij}$ be the generic vector of local measurement(s) associated with the individual j-th sensor of the i-th measurement system. In general, $\mathbf{S}_{ij}$ can be of three types:

- $\mathbf{S}_{ij} = \left[\hat{d}_{ij} \right]$ for sensors performing distance measurements only (for instance, ADMs, interferometers, ultrasound sensors, etc.), where $\hat{d}_{ij}$ is the local distance measurement. These sensors generally equip LVM systems based on multilateration (Franceschini et al., 2011);

- $\mathbf{S}_{ij} = \left[\hat{\theta}_{ij}, \hat{\varphi}_{ij} \right]$ for angular sensors (for instance, optical/magnetical encoders, photogrammetric cameras, iGPS sensors, etc.), where $\hat{\theta}_{ij}$ and $\hat{\varphi}_{ij}$ are respectively the local measurements of the azimuth and elevation angles. These sensors generally equip LVM systems based on triangulation (Franceschini et al., 2011; Caja et al., 2015);

- $\mathbf{S}_{ij} = \left[\hat{d}_{ij}, \hat{\theta}_{ij}, \hat{\varphi}_{ij} \right]$ for hybrid sensors, i.e. sensors able to measure one distance and two angles (for instance, laser trackers, 3D scanners, or combinations of other sensors). These sensors generally equip hybrid LVM systems (Franceschini et al., 2011);

Let also $\Sigma_{\mathbf{S}_{ij}}$ be the covariance matrix related to each sensor measurement.

The competitive approach (schematized in Figure 5a) estimates the position of P, relying on the position estimates performed by the individual systems and the relevant uncertainties:

$$\hat{\mathbf{X}}_{P,COMP} = f_{COMP}\left(\hat{\mathbf{X}}_{P_i} \middle| \Sigma_{\hat{\mathbf{X}}_{P_i}} \quad \forall i \in \{1,...,N\} \right), \tag{7}$$

On the other hand, the cooperative approach (schematized in Figure 5b) estimates the position of P, relying on the local angular and distance measurements, performed by the individual sensors and the relevant uncertainties:

$$\hat{\mathbf{X}}_{P,COOP} = f_{COOP}\left(\mathbf{S}_{ij} \middle| \Sigma_{\mathbf{S}_{ij}} \quad \forall (i,j): i \in \{1,...,N\}, j \in \{1,...,M_i\} \right), \tag{8}$$
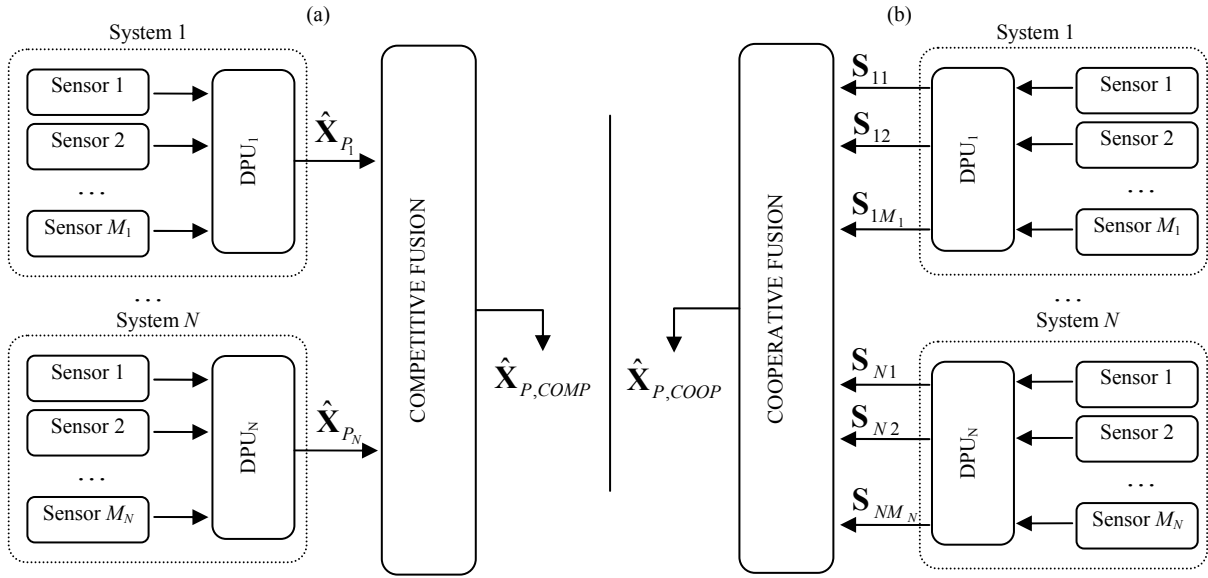
Figure 5. Schematic representation of the two possible data-fusion approaches, i.e. (a) competitive and (b) cooperative approach.

4. Discussion of the two data-fusion approaches

The following two sub-sections provide a detailed discussion of the competitive and cooperative fusion approaches, respectively.

4.1 Competitive data-fusion approach

The competitive approach is relatively simple to formalize, using the notation introduced in Sect. 3. Let $\mathbf{A}$ be a 3Nx3 matrix defined as $\mathbf{A} = [\mathbf{I}_{3,3} \quad \mathbf{I}_{3,3} \quad \dots \quad \mathbf{I}_{3,3}]^T$, in which $\mathbf{I}_{3,3}$ is the 3x3 identity matrix. Defining $\mathbf{b}$ as $\mathbf{b} = [\hat{\mathbf{X}}_{P_1}^T \quad \hat{\mathbf{X}}_{P_2}^T \quad \cdots \quad \hat{\mathbf{X}}_{P_N}^T]^T$, the estimation of the position of P ($\hat{\mathbf{X}}_{P,COMP}$) can be obtained by reversing the relationship:

$$\mathbf{A}\mathbf{X}_{P,COMP} = \mathbf{b} . \tag{9}$$

Since this system is overdefined (3N equations in 3 unknown parameters, i.e. the 3 coordinates of $\mathbf{X}_{P,COMP}$), there are several possible solution approaches, ranging from those based on the iterative minimization of a suitable error function (Franceschini et al., 2011), to those based on the Least Squares method (Wolberg, 2005). To this purpose, the most elegant and practical approach is probably that of the Generalized Least Squares (GLS) method (Kariya and Kurata, 2004), in which a weight matrix ($\mathbf{W}$), which takes into account the uncertainty produced by the equations of the system, is defined. One of the most practical ways to define this matrix is the application of the Multivariate Law of Propagation of Uncertainty (MLPU) to the random variable in Eq. (9), i.e. $\mathbf{b}$. By applying the GLS method to the system in Eq. (9), we obtain the position estimate of P as:

$$\hat{\mathbf{X}}_{P,COMP} = (\mathbf{A}^T\mathbf{W}\mathbf{A})^{-1}\mathbf{A}^T\mathbf{W}\mathbf{b} , \tag{10}$$

where $\mathbf{W}$ is the weighting matrix that – under the hypothesis of independence between the

9

measurements provided by different systems – is defined as:

$$\mathbf{W} = \begin{bmatrix} \Sigma_{\hat{\mathbf{X}}_{P_1}} & \mathbf{0} & \cdots & \mathbf{0} \\ \mathbf{0} & \Sigma_{\hat{\mathbf{X}}_{P_2}} & \cdots & \mathbf{0} \\ \vdots & \vdots & \ddots & \vdots \\ \mathbf{0} & \mathbf{0} & \cdots & \Sigma_{\hat{\mathbf{X}}_{P_N}} \end{bmatrix}^{-1}$$
(11)

and $\mathbf{0}$ is the 3x3 null matrix.

Please notice that Eq. (10) is the most compact form to express the inversion of Eq. (9), however, it is not the most convenient approach to calculate $\hat{\mathbf{X}}_{P,COMP}$. For instance, rather than considering the inverse of $\mathbf{W}$, one could take the inverse of each $\Sigma_{\hat{\mathbf{X}}_{P_i}}$ since $\mathbf{W}$ is a block diagonal matrix. Similar considerations holds for Eqs. (12) and (36).

4.2. Cooperative data-fusion approach

The problem of cooperative data-fusion is more complicated. As for the competitive approach, an estimation of the position of P ($\hat{\mathbf{X}}_{P,COOP}$) can be obtained by reversing the linear system:

$$\mathbf{C}\mathbf{X}_{P,COOP} = \mathbf{q},$$
(12)

where $\mathbf{C}$ and $\mathbf{q}$ are respectively the design matrix and the observation vector, which may depend on the specific LVM systems and the relevant sensors in use. Precisely, the design matrix and the observation vector have the following form:

$$\mathbf{C} = \begin{bmatrix} \begin{bmatrix} \mathbf{C}_{11} \\ \vdots \\ \mathbf{C}_{1M_1} \end{bmatrix} \\ \vdots \\ \begin{bmatrix} \mathbf{C}_{N1} \\ \vdots \\ \mathbf{C}_{NM_N} \end{bmatrix} \end{bmatrix}, \quad \mathbf{q} = \begin{bmatrix} \begin{bmatrix} \mathbf{q}_{11} \\ \vdots \\ \mathbf{q}_{1M_1} \end{bmatrix} \\ \vdots \\ \begin{bmatrix} \mathbf{q}_{N1} \\ \vdots \\ \mathbf{q}_{NM_N} \end{bmatrix} \end{bmatrix}.$$
(13)

The following sub-sections discuss the definition of the generic $\mathbf{C}_{ij}$ matrix and $\mathbf{q}_{ij}$ vector, depending on the sensor type and show a practical solution to the problem in Eq. 12.

4.2.1 Distance Sensors (Multi-lateration)

When the j-th sensor of the i-th system is a distance sensor, $\mathbf{C}_{ij}$ and $\mathbf{q}_{ij}$ are defined as follows.

Each j-th sensor of the i-th system is able to estimate the distance from its position ($\mathbf{X}_{\mathbf{0}_{ij}}$) to P ($\mathbf{X}_P$). Consistently with the notation introduced in Sect.3 and neglecting the sensors' local measurement errors, this distance estimate can be expressed as:

$$\hat{d}_{ij} = \left\| \mathbf{X}_P - \mathbf{X}_{0_{ij}} \right\| = \sqrt{\left(X - X_{O_{ij}}\right)^2 + \left(Y - Y_{O_{ij}}\right)^2 + \left(Z - Z_{O_{ij}}\right)^2}. \tag{14}$$

Squaring both terms, we obtain

$$\left(X - X_{O_{ij}}\right)^2 + \left(Y - Y_{O_{ij}}\right)^2 + \left(Z - Z_{O_{ij}}\right)^2 - \hat{d}_{ij}^2 = 0. \tag{15}$$

Function in Eq. (15) can be linearized by means of its first order Taylor series expansion around a generic point $\mathbf{X_A} = [X_A, Y_A, Z_A]^T$. Therefore, a linear approximation of Eq. 15 is given by the sum of (i) Eq. 15 evaluated in $\mathbf{X_A}$ and (ii) the gradient of Eq. 15 with respect to $\mathbf{X}$ evaluated in $\mathbf{X_A}$, multiplied by $(\mathbf{X} - \mathbf{X_A})$:

$$\left(X_A - X_{O_{ij}}\right)^2 + \left(Y_A - Y_{O_{ij}}\right)^2 + \left(Z_A - Z_{O_{ij}}\right)^2 - \hat{d}_{ij}^2 + 2\begin{bmatrix} X_A - X_{O_{ij}} \\ Y_A - Y_{O_{ij}} \\ Z_A - Z_{O_{ij}} \end{bmatrix}^T \cdot \begin{bmatrix} X - X_A \\ Y - Y_A \\ Z - Z_A \end{bmatrix} \approx 0. \tag{16}$$

$\mathbf{X_A}$ act as a first approximation of $\mathbf{X}_P$. The approximation in Eq. (16) gets better and better the closer $\mathbf{X_A}$ is to $\mathbf{X}_P$.

In matrix form, Eq. (16) becomes:

$$\mathbf{C}_{ij}\mathbf{X} = \mathbf{q}_{ij}, \tag{17}$$

where

$$\begin{aligned} \mathbf{C}_{ij} &= 2\left\lfloor X_A - X_{O_{ij}} \quad Y_A - Y_{O_{ij}} \quad Z_A - Z_{O_{ij}} \right\rfloor \\ \mathbf{q}_{ij} &= \hat{d}_{ij}^2 + X_A^2 - X_{0_{ij}}^2 + Y_A^2 - Y_{0_{ij}}^2 + Z_A^2 - Z_{0_{ij}}^2 \end{aligned}. \tag{18}$$

Being Eq. (17) the linearization of Eq. (15), only an approximated value of $\mathbf{X}_P$ can be obtained by reversing Eq. 17. An iterative solution of Eq. (17) can be obtained according to the following procedure:

1. Define a preliminary value of $\mathbf{X_A}$ (close to the true value of $\mathbf{X}_P$)

2. Solve for $\mathbf{X}_P$ by reversing Eq. (17)

3. If $\mathbf{X}_P$ is reasonably close to $\mathbf{X_A}$ then

4.   Go to Step 9

5. Else

6.   Set $\mathbf{X_A}$ as the obtained approximation of $\mathbf{X}_P$.

7.   Go To Step 2

8. End if

9. End

4.2.2 Angular Sensors (Triangulation)

If the *j*-th sensor of the *i*-th system is an angular sensor, $\mathbf{C}_{ij}$ and $\mathbf{q}_{ij}$ are defined as follows.

From the local perspective of each sensor, two angles – i.e., θ_{ij} (azimuth) and φ_{ij} (elevation) – are subtended by the line passing through P and a local *observation point*, which we assume as coincident with the origin $o_i \equiv [0,0,0]$ of the local coordinate system (see Figure 6).
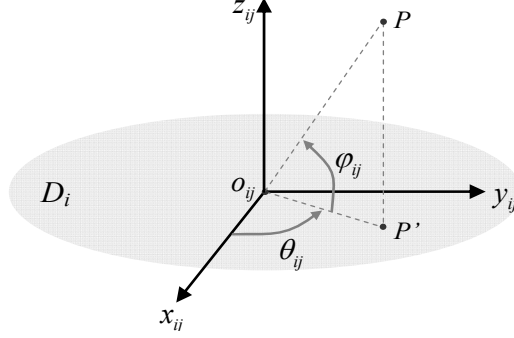
Figure 6. For a generic network device (D_i), two angles – i.e., θ_{ij} (azimuth) and φ_{ij} (elevation) – are subtended by a line joining the point P (to be localized) and the origin o_{ij} of the local coordinate system o_{ij}-$x_{ij}y_{ij}z_{ij}$.

Precisely, φ_{ij} describes the inclination of segment $o_{ij}P$ with respect to the plane $x_{ij}y_{ij}$ (with a positive sign when $z_{ij}>0$), while θ_{ij} describes the counterclockwise rotation of the projection ($o_{ij}P'$) of $o_{ij}P$ on the $x_{ij}y_{ij}$ plane, with respect to the x_{ij} axis. If we consider the angular measurements ($\hat{\theta}_{ij}, \hat{\varphi}_{ij}$) and we neglect measurement errors, the following relationships hold for each i-th local coordinate system:

$$\tan \hat{\theta}_{ij} = \frac{y_{ij}}{x_{ij}} \qquad \begin{cases} \text{if } x_{ij} \geq 0 \text{ then } -\frac{\pi}{2} \leq \hat{\theta}_{ij} \leq \frac{\pi}{2} \\ \text{if } x_{ij} < 0 \text{ then } \frac{\pi}{2} < \hat{\theta}_{ij} < \frac{3\pi}{2} \end{cases} \tag{19}$$

$$\sin \hat{\varphi}_{ij} = \frac{z_{ij} \cos \hat{\theta}_{ij} \cos \hat{\varphi}_{ij}}{x_{ij}} \qquad \left\{ -\frac{\pi}{2} \leq \hat{\varphi}_{ij} \leq \frac{\pi}{2} \right.$$

Eq. (19) can be reformulated as:

$$\begin{bmatrix} \sin \hat{\theta}_{ij} & -\cos \hat{\theta}_{ij} & 0 \\ \sin \hat{\varphi}_{ij} & 0 & -\cos \hat{\theta}_{ij} \cos \hat{\varphi}_{ij} \end{bmatrix} \mathbf{x}_{ij} = 0. \tag{20}$$

Reversing Eq. (5) we have

$$\mathbf{R}_{ij}^T \mathbf{X} = \mathbf{x}_{ij} + \mathbf{R}_{ij}^T \mathbf{X}_{0_{ij}}. \tag{21}$$

Combining Eq. (20) and (21), one can obtain:

$$\begin{bmatrix} \sin \hat{\theta}_{ij} & -\cos \hat{\theta}_{ij} & 0 \\ \sin \hat{\varphi}_{ij} & 0 & -\cos \hat{\theta}_{ij} \cos \hat{\varphi}_{ij} \end{bmatrix} \mathbf{R}_{ij}^T \mathbf{X} = \begin{bmatrix} \sin \hat{\theta}_{ij} & -\cos \hat{\theta}_{ij} & 0 \\ \sin \hat{\varphi}_{ij} & 0 & -\cos \hat{\theta}_{ij} \cos \hat{\varphi}_{ij} \end{bmatrix} \mathbf{R}_{ij}^T \mathbf{X}_{0_{ij}}. \tag{22}$$

which can be written as:

$$\mathbf{C}_{ij} \mathbf{X} = \mathbf{q}_{ij}, \tag{23}$$

where $\mathbf{q}_{ij} = \mathbf{C}_{ij} \cdot \mathbf{X}_{0_{ij}}$ and

$$\mathbf{C}_{ij} = \begin{bmatrix} \sin\hat{\theta}_{ij} & -\cos\hat{\theta}_{ij} & 0 \\ \sin\hat{\varphi}_{ij} & 0 & -\cos\hat{\theta}_{ij}\cos\hat{\varphi}_{ij} \end{bmatrix} \cdot \mathbf{R}_{ij}^{T}. \tag{24}$$

4.2.3 Hybrid Approach

When a generic sensor is able to perform both distance and angular measurements (i.e. providing $\hat{d}_{ij}, \hat{\theta}_{ij}$ and $\hat{\varphi}_{ij}$), the problem is relatively simple. Neglecting measurement errors, the following relationships hold:

$$\begin{cases} x_{ij} = \hat{d}_{ij}\cos\hat{\varphi}_{ij}\cos\hat{\theta}_{ij} \\ y_{ij} = \hat{d}_{ij}\cos\hat{\varphi}_{ij}\sin\hat{\theta}_{ij} \\ z_{ij} = \hat{d}_{ij}\sin\hat{\varphi}_{ij} \end{cases}. \tag{25}$$

Combining Eqs. (5) and (25) we obtain:

$$\mathbf{R}_{ij}^{T}\mathbf{X} - \mathbf{R}_{ij}^{T}\mathbf{X}_{\mathbf{0}_{ij}} = \begin{bmatrix} \hat{d}_{ij}\cos\hat{\varphi}_{ij}\cos\hat{\theta}_{ij} & \hat{d}_{ij}\cos\hat{\varphi}_{ij}\sin\hat{\theta}_{ij} & \hat{d}_{ij}\sin\hat{\varphi}_{ij} \end{bmatrix}^{T}. \tag{26}$$

Eq. (26) can be reformulated as:

$$\mathbf{C}_{ij}\mathbf{X} = \mathbf{q}_{ij}, \tag{27}$$

where $\mathbf{C}_{ij} = \mathbf{R}_{ij}^{T}$, $\mathbf{q}_{ij} = \mathbf{t}_{ij} + \mathbf{R}_{ij}^{T}\mathbf{X}_{\mathbf{0}_{ij}}$ and $\mathbf{t}_{ij} = \begin{bmatrix} \hat{d}_{ij}\cos\hat{\varphi}_{ij}\cos\hat{\theta}_{ij} & \hat{d}_{ij}\cos\hat{\varphi}_{ij}\sin\hat{\theta}_{ij} & \hat{d}_{ij}\sin\hat{\varphi}_{ij} \end{bmatrix}^{T}$.

4.2.4 Weighting and Solution

In order to solve Eq. (12) for $\hat{\mathbf{X}}_{P,COOP}$, a GLS approach can be adopted. To this purpose, it is convenient to define a weight matrix that is inversely proportional to the variability of the error vector $\mathbf{u}$:

$$\mathbf{u} = \mathbf{C}\hat{\mathbf{X}}_{P,COOP} - \mathbf{q}. \tag{28}$$

Notice that $\mathbf{u}$ is not only a function of $\hat{\mathbf{X}}_{P,COOP}$ but it also depends on the sensors' local measurements and intrinsic parameters (i.e., $\mathbf{X}_{\mathbf{0}_{ij}}$, ω_{ij}, ϕ_{ij} and κ_{ij},). For simplicity we neglect here the uncertainty in the estimation of the intrinsic parameters, which is generally obtained by a suitable calibration process (Mastrogiacomo and Maisano, 2010). Defining the overall measurement vector as:

$$\mathbf{S} = \begin{bmatrix} \begin{bmatrix} \mathbf{S}_{11} \\ \vdots \\ \mathbf{S}_{1M_1} \end{bmatrix} \\ \vdots \\ \begin{bmatrix} \mathbf{S}_{N1} \\ \vdots \\ \mathbf{S}_{NM_N} \end{bmatrix} \end{bmatrix}, \tag{29}$$

the GLS weighting matrix ($\mathbf{\Omega}$) can be obtained applying the MLPU to $\mathbf{u}$ (BIPM et al., 2008):

$$\mathbf{\Omega} = \left(\mathbf{J}_{\mathbf{u}(S)} \operatorname{cov}(S) \mathbf{J}_{\mathbf{u}(S)}^T\right)^{-1}, \tag{30}$$

Where $\mathbf{J}_{\mathbf{u}(S)}$ is the Jacobian matrix of $\mathbf{u}$ with respect to $\mathbf{S}$. Assuming sensors to be independent from each other, $\mathbf{\Omega}$ will be a block diagonal matrix:

$$\mathbf{\Omega} = \begin{bmatrix} \begin{bmatrix} \mathbf{\Omega}_{11} & \mathbf{0} & \mathbf{0} \\ \mathbf{0} & \ddots & \mathbf{0} \\ \mathbf{0} & \mathbf{0} & \mathbf{\Omega}_{1M_1} \end{bmatrix} & \cdots & \mathbf{0} \\ \vdots & \ddots & \vdots \\ \mathbf{0} & \cdots & \begin{bmatrix} \mathbf{\Omega}_{N1} & \mathbf{0} & \mathbf{0} \\ \mathbf{0} & \ddots & \mathbf{0} \\ \mathbf{0} & \mathbf{0} & \mathbf{\Omega}_{NM_N} \end{bmatrix} \end{bmatrix}. \tag{31}$$

where the generic sub-matrix $\mathbf{\Omega}_{ij}$ depends on the type of sensor. Precisely, if $\mathbf{S}_{ij} = \left[\hat{d}_{ij}\right]$, $\mathbf{\Omega}_{ij}$ is given by:

$$\mathbf{\Omega}_{ij} = \left(\mathbf{J}_{ij} \operatorname{cov}(\mathbf{S}_{ij}) \mathbf{J}_{ij}^T\right)^{-1}. \tag{32}$$

being

$$\begin{cases} \mathbf{J}_{ij} = \left(2d_{ij}\right) \\ \operatorname{cov}(\mathbf{S}_{ij}) = \sigma_{d_{ij}}^2 \end{cases}. \tag{33}$$

If $\mathbf{S}_{ij} = \left[\hat{\theta}_{ij}, \hat{\varphi}_{ij}\right]$, $\mathbf{\Omega}_{ij}$ is again given by Eq. (32) being

$$\begin{cases} \mathbf{J}_{ij} = \begin{bmatrix} x_{ij} \cos\theta_{ij} + y_{ij} \sin\theta_{ij} & 0 \\ z_{ij} \sin\theta_{ij} \cos\varphi_{ij} & x_{ij} \cos\varphi_{ij} + z_{ij} \cos\theta_{ij} \sin\varphi_{ij} \end{bmatrix} \\ \operatorname{cov}(\mathbf{S}_{ij}) = \begin{bmatrix} \sigma_{\theta_{ij}}^2 & 0 \\ 0 & \sigma_{\varphi_{ij}}^2 \end{bmatrix} \end{cases}. \tag{34}$$

If $\mathbf{S}_{ij} = \left[\hat{d}_{ij}, \hat{\theta}_{ij}, \hat{\varphi}_{ij}\right]$, $\mathbf{\Omega}_{ij}$ is given by Eq. (32) being

$$\begin{cases} \mathbf{J}_{ij} = \begin{bmatrix} \cos\varphi_{ij} \cos\theta_{ij} & -d_{ij} \cos\varphi_{ij} \sin\theta_{ij} & -d_{ij} \sin\varphi_{ij} \cos\theta_{ij} \\ \cos\varphi_{ij} \sin\theta_{ij} & d_{ij} \cos\varphi_{ij} \cos\theta_{ij} & -d_{ij} \sin\varphi_{ij} \sin\theta_{ij} \\ \sin\varphi_{ij} & 0 & d_{ij} \cos\varphi_{ij} \end{bmatrix} \\ \operatorname{cov}(\mathbf{S}_{ij}) = \begin{bmatrix} \sigma_{d_{ij}}^2 & 0 & 0 \\ 0 & \sigma_{\theta_{ij}}^2 & 0 \\ 0 & 0 & \sigma_{\varphi_{ij}}^2 \end{bmatrix} \end{cases}. \tag{35}$$

Having defined Ω, Eq. (12) can be reversed as:

$$\hat{\mathbf{X}}_{P,COOP} = \left(\mathbf{C}^T \mathbf{\Omega} \mathbf{C}\right)^{-1} \mathbf{C}^T \mathbf{\Omega} \mathbf{q}. \tag{36}$$

Note that $\operatorname{cov}(\mathbf{S}_{ij})$ is diagonal since sensors are assumed to be independent to each other. This is a

reasonable assumption since the sensors operate independently during measuring operations. However, external factors – such as accidental vibrations, thermal gradients, etc. – may cause correlation between measures of separate sensors. In this case the assumption can be relaxed simply by inserting the non-diagonal elements in the matrix, if they can be estimated.

5. Test Bench Comparison

The purpose of this section is to compare by simulations the two fusion approaches on two practical case-studies: (i) combination of a set of LTs (i.e. equipped with hybrid sensors) and (ii) combination of measuring system based on triangulation (i.e. equipped with angular sensors) and multi-lateration (i.e. equipped with distance sensors). Also, the results of some preliminary experiments are presented.

5.1 Combination of LTs

In this case-study, we simulate an industrial-like environment where a set of LTs are used to measure the position of several points of interest. In practice, LTs are generally positioned at a sufficiently large distance from the points to be measured, in order to "cover" the largest possible measurement volume. Moreover, they are sturdy placed on isostatic tripods, which can be adjusted in height.

In the simulations, the LTs are distributed according to in an area of 20m x 20m with a variable height between 1 and 2m and with their vertical axis orthogonal to the floor plan. . As an example see Figure 7.

The number of LTs is varied from 2 to 10, and 30 different layouts are generated for each case; 9x30 = 270 total layouts are generated. For each of these layouts, we generate 1000 total points uniformly distributed in the measurement volume.
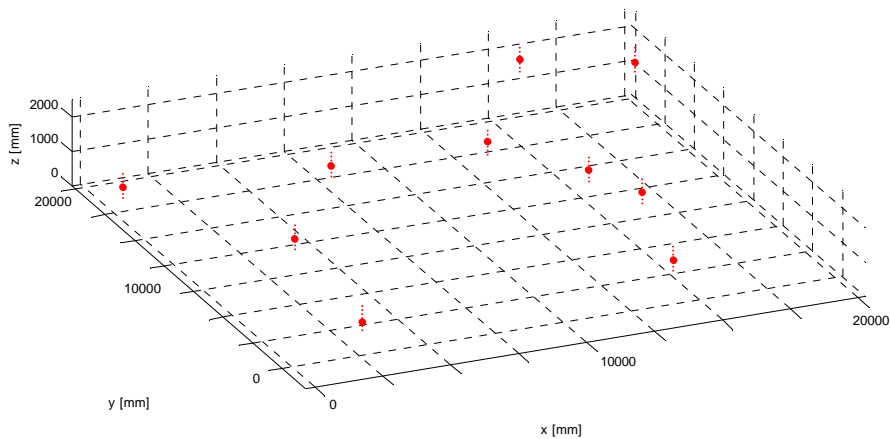
Figure 7. Example of simulated layout with 10 LTs. Circles and dotted lines represent respectively the positions and axis orientations of the LTs.

For each point and each *j*-th sensor, distance and angular measurements $(\hat{d}_{ij}, \hat{\theta}_{ij}, \hat{\varphi}_{ij})$ are simulated

by adding a zero-mean Gaussian noise to the relevant "true" values (i.e. d_{ij}, θ_{ij} and φ_{ij}); these "true" values are exactly calculated knowing the relative positions of the sensors with respect to the point of interest (angles in degrees and distances in mm):

$$
\begin{aligned}
\hat{d}_{ij} &= d_{ij} + \varepsilon_d &\text{with}&& \varepsilon_d &\sim \mathrm{N}(0, \sigma_d = 2.5 \cdot d_{j,i} \cdot 10^{-3}) \\
\hat{\theta}_{ij} &= \theta_{ij} + \varepsilon_\theta &\text{with}&& \varepsilon_\theta &\sim \mathrm{N}(0, \sigma_\theta = 8 \cdot 10^{-4}) \\
\hat{\varphi}_{ij} &= \varphi_{ij} + \varepsilon_\varphi &\text{with}&& \varepsilon_\varphi &\sim \mathrm{N}(0, \sigma_\varphi = 8 \cdot 10^{-4})
\end{aligned}
\tag{37}
$$

The above measurements are assumed to be uncorrelated and the standard deviations of the Gaussian noise are consistent with the typical uncertainties in distance and angular measurements by LTs, as reported in the scientific literature (Calkins and Salerno, 2000).

The position of the points of interest is estimated through the competitive and cooperative approaches.

In order to apply the cooperative approach, the measurement uncertainties of the sensors (in the form of σ_d, σ_θ and σ_φ) are assumed to be known.

Regarding the competitive approach, coordinates measurement uncertainty ($\Sigma_{\hat{\mathbf{x}}_{P_i}}$) was estimated using a Montecarlo simulation with 1000 replications for each point.

Error in the localization is analyzed by comparing the simulated localization ($\hat{\mathbf{X}}_P$) with the nominal positions ($\mathbf{X}$). To this purpose, the absolute localization error is defined as:

$$
\mathrm{e} = \left\| \mathbf{X} - \hat{\mathbf{X}}_P \right\|.
\tag{38}
$$

Results are summarized in Figure 8 and Table 1. In detail, Figure 8 shows multiple boxplots of the localization error (e) against the number of LTs in use. As expected, increasing the number of LTs results in a reduction of both the localization error and its uncertainty.
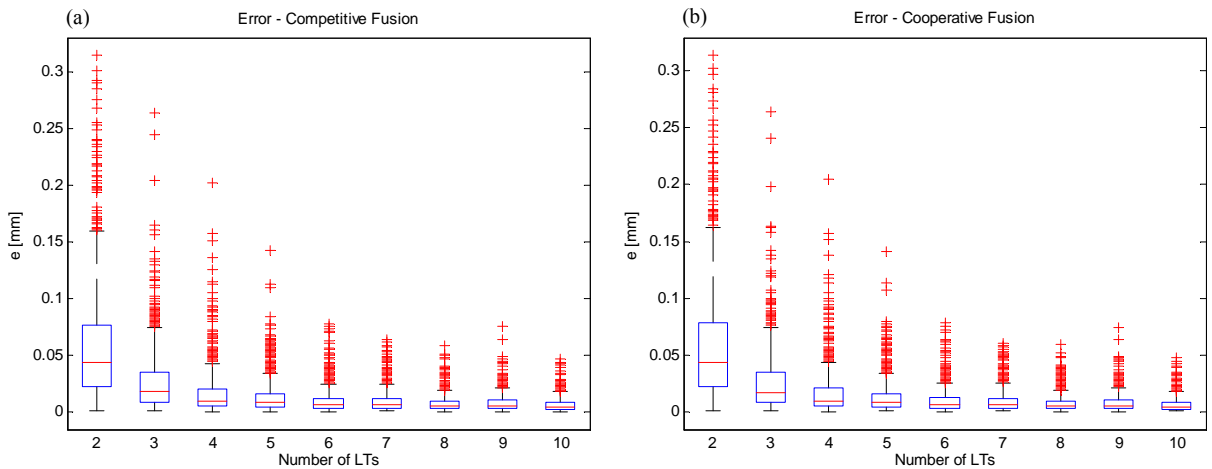
Figure 8. Boxplot of the localization error against the number of LTs in use: (a) competitive and (b) cooperative fusion approach. On each box, the central mark is the median, the edges of the box are the 25th and 75th

percentiles, the whiskers extend to the most extreme data points, which are not considered as outliers; outliers are plotted individually.

Table 1 provides a quantitative synthesis of the simulation results. The analyses of the mean value and the 25th and 75th percentiles of the localization error show non-significant differences between the two approaches.

Table 1. Mean value, 25th and 75th percentiles (Q1 and Q3) of the localization error distribution. Comparison between cooperative and competitive fusion approaches (values in mm).

No. of LTs	Cooperative			Competitive		
	Mean	Q1	Q3	Mean	Q1	Q3
2	0.0438	0.0219	0.0771	0.0438	0.0222	0.0783
3	0.0173	0.0082	0.0352	0.0176	0.0082	0.0348
4	0.0098	0.0051	0.0204	0.0099	0.0052	0.0208
5	0.0087	0.0045	0.0162	0.0087	0.0045	0.0162
6	0.0063	0.0035	0.0121	0.0064	0.0035	0.0122
7	0.0063	0.0033	0.0120	0.0062	0.0033	0.0120
8	0.0053	0.0030	0.0093	0.0053	0.0030	0.0094
9	0.0052	0.0029	0.0102	0.0052	0.0029	0.0104
10	0.0044	0.0025	0.0087	0.0044	0.0025	0.0088

The great similarity between the results obtained through the two approaches is probably due to the fact that, for each LT, the position of P is determined uniquely, with no redundant information (i.e., three local measurements correspond to the three unknown coordinates of P).

5.2 Combination of triangulation and multilateration systems

The second case study analyses the combination between two distributed LVM systems based on triangulation and multilateration respectively. For example, this can be the case of the combination of a photogrammetric system (based on triangulation) with a set of interferometers (based on multilateration).

In the simulations, sensors are uniformly distributed in an area of 20m x 20m at variable height between 2m and 3m (for the triangulation system) and 1m and 2m (for multilateration system). Both triangulation and multilateration sensors are oriented with vertical axis orthogonal to the floor plan.

The number of sensors of each system is varied from 4 to 10, generating 30 different layouts for each case. Total 7x7x30 = 1470 different layouts are generated. For each layout, total 1000 points uniformly distributed over the measurement volume are generated.
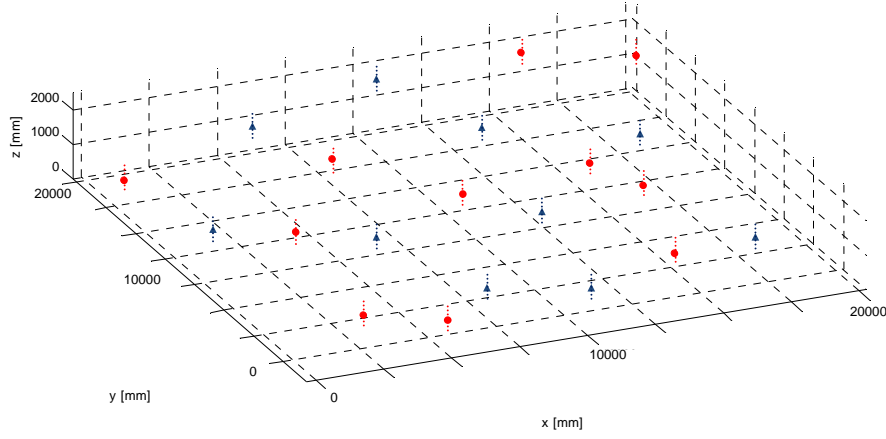
Figure 9. Example of simulated layout with 10 triangulation (circles) and 10 multilateration (triangles) sensors. Dotted lines represent sensors' orientation axis.

Distance measurements ($\hat{d}_{ij}$) are simulated by adding a Gaussian noise to the true value (i.e. d_{ij}), exactly calculated according to the relative positions between sensors and points (distances in mm):

$$\hat{d}_{ij} = d_{ij} + \varepsilon_d \quad with \quad \varepsilon_d \sim \mathrm{N}(0, \sigma_d = 2.5 \cdot d_{ij} \cdot 10^{-3}). \tag{39}$$

Azimuth and elevation measurements of ($\hat{d}_{ij}, \hat{\theta}_{ij}, \hat{\varphi}_{ij}$) are simulated by adding a zero-mean Gaussian noise to the relevant true value (i.e. d_{ij}, θ_{ij} and φ_{ij}), which is calculated knowing the position of the sensors with respect to the points of interest (angles in degrees):

$$\begin{aligned}
\hat{\theta}_{ij} &= \theta_{ij} + \varepsilon_\theta \quad with \quad \varepsilon_\theta \sim \mathrm{N}(0, \sigma_\theta = 3 \cdot 10^{-3}) \\
\hat{\varphi}_{ij} &= \varphi_{ij} + \varepsilon_\varphi \quad with \quad \varepsilon_\varphi \sim \mathrm{N}(0, \sigma_\varphi = 3 \cdot 10^{-3})
\end{aligned} \tag{40}$$

The above measures are assumed to be uncorrelated and the standard deviations of the Gaussian noise are consistent with the typical uncertainties in angular measurements by photogrammetric cameras, as reported in the scientific literature (Franceschini et al., 2011).

The position of the points of interest is estimated through the competitive and cooperative approaches.

In order to apply the cooperative approach, the measurements uncertainties of the sensors (in the form of σ_d, σ_θ and σ_φ) are assumed to be known. Regarding the competitive approach, the standard deviations relating to the position of *P* are estimated through a Montecarlo simulation with 1000 replications for each point.

As for the simulations described in Sect. 5.1, results are analyzed by comparing the result of the simulated localization ($\hat{\mathbf{X}}_P$) with the "true" nominal positions ($\mathbf{X}$), by means of the absolute localization error (see Eq. (38)). Results are summarized in Table 2, which shows the average value of the localization error (e) for the different layouts tested. Table A.1 (in the Appendix) is the extended version of Table 2, including the 25th and 75th percentiles of the error distribution. The analysis of these results suggests the following considerations:

18

- The localization uncertainty tends to decrease when increasing the number of sensors. In particular, there seems to be an asymptotical decreasing trend. For the purpose of example, Figure 8 shows the results of the cooperative fusion, when the number of angular sensors is fixed to 7.
- The cooperative approach is systematically slightly better than the competitive one in terms of localization uncertainty. This aspect is also evident in Table A.1 (in the Appendix) where the interquartile range (i.e., the gap between the 25th and 75th percentiles) is systematically lower in the case of the cooperative approach.

Table 2. Mean value of the localization error [mm] for the different layouts tested. The results obtained by competitive ("Comp.") and cooperative ("Coop.") approaches are reported. Table A.1 (in the Appendix) is the extended version of this table.

		Number of distance sensors												
		4		5		6		7		8		9		10	
		Comp.	Coop.	Comp.	Coop.	Comp.	Coop.	Comp.	Coop.	Comp.	Coop.	Comp.	Coop.	Comp.	Coop.
Number of angular sensors	4	0.0192	0.0189	0.0152	0.0151	0.0111	0.0110	0.0096	0.0095	0.0085	0.0085	0.0077	0.0077	0.0064	0.0064
	5	0.0189	0.0188	0.0129	0.0129	0.0106	0.0106	0.0095	0.0094	0.0088	0.0088	0.0073	0.0072	0.0073	0.0073
	6	0.0199	0.0197	0.0141	0.0140	0.0121	0.0120	0.0096	0.0096	0.0086	0.0085	0.0075	0.0075	0.0069	0.0069
	7	0.0209	0.0205	0.0139	0.0137	0.0119	0.0118	0.0097	0.0096	0.0084	0.0084	0.0073	0.0073	0.0067	0.0066
	8	0.0186	0.0183	0.0136	0.0136	0.0123	0.0123	0.0095	0.0095	0.0082	0.0081	0.0075	0.0075	0.0069	0.0069
	9	0.0189	0.0186	0.0151	0.0150	0.0111	0.0110	0.0090	0.0090	0.0083	0.0083	0.0077	0.0076	0.0070	0.0070
	10	0.0184	0.0181	0.0129	0.0127	0.0101	0.0100	0.0088	0.0087	0.0080	0.0080	0.0080	0.0079	0.0064	0.0064
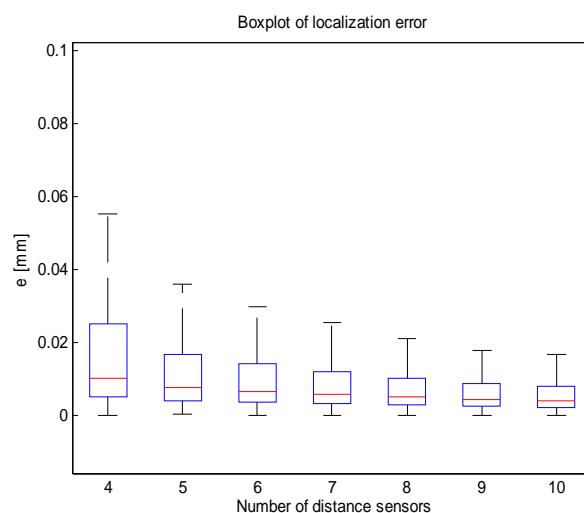
Figure 10. Boxplot of the localization error against the number of distance sensors, when applying the cooperative approach. On each box, the central mark is the median, the edges of the box are the 25th and 75th percentiles, the whiskers extend to the most extreme data points, not considered as outliers.

5.3 Preliminary experiments

The two approaches have been implemented considering a specific combination of two LVM

systems: (i) a photogrammetric system (PS) OptiTrack V120-TRIOTM (NaturalPoint, 2015) equipped with 38.1 mm reflective spherical markers, and (ii) a laser tracker (LT) API RadianTM (API Automated Precision INC., 2015). The experiments have been conducted in the laboratories of Microservice S.r.l., which also provided the LT.

The PS consists of a set of 3 cameras fixed on a line frame (see Figure 9), each of which is able to provide an azimuth ($\hat{\theta}_{PS}$) and elevation ($\hat{\varphi}_{PS}$) measurement of the target point. Using these data, the PS is able to estimate the position of each measured point P (NaturalPoint, 2015).

The LT is equipped with an absolute distance meter (ADM) or a laser interferometer (measuring distances ($\hat{d}_{LT}$)) and angular encoders (measuring azimuth ($\hat{\theta}_{LT}$) and elevation ($\hat{\varphi}_{LT}$) angles). Using these data, the LT is able to automatically estimate the position of measured points (API Automated Precision INC., 2015).

When implementing the cooperative approach, the 3D position of each measured point is obtained using the local distance and angular measurements, performed by the sensors equipping the two systems (i.e. $\hat{\theta}_{PS}$ and $\hat{\varphi}_{PS}$, for each camera of the PS, and $\hat{d}_{LT}$, $\hat{\theta}_{LT}$ and $\hat{\varphi}_{LT}$, for the LT).
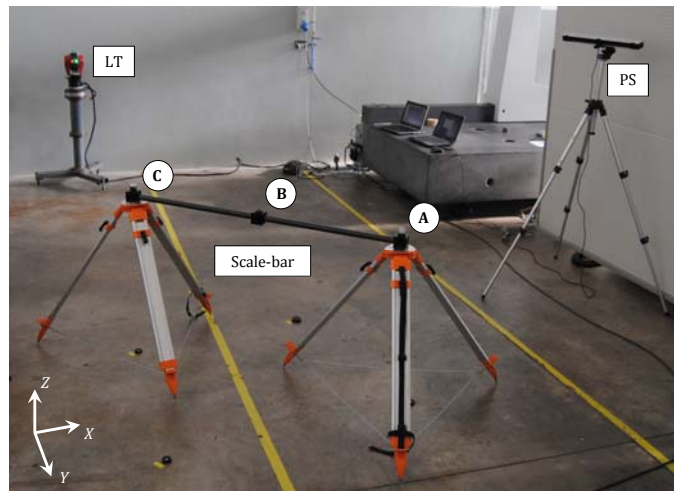
Figure 11. Measurement layout (A, B and C are the reference points of the scale-bar).

To obtain an optimal alignment between the coordinate systems of the LT and the PS, 18 points, randomly distributed in the measuring volume, have been measured by both the LVM systems (Durrant-Whyte, 1988; Haghighat et al., 2011).

The layout of the two systems is reported in Figure 11, which also shows the scale-bar used for the experiment. Distance values among the reference markers on the scale-bar were calibrated on a Coordinate Measuring Machine (CMM – DEA Iota0101).

The position measurement of three points on the scale bar has been replicated 30 time to obtain the results in Table 2. The mean value of the distances measured on the scale-bar and the related standard deviations are reported, for all the possible sensor configurations. Results are compared with those obtained using (i) the LT and the PS individually and (ii) the competitive approach

implemented by the SpatialAnalyser® software (New River Kinematics, 2015).

Table 2. Distances measured on the scale-bar, using different sensor configurations (values reported in mm)

Config.	d_{A-B}	$\sigma_{d_{A-B}}$	d_{B-C}	$\sigma_{d_{B-C}}$	d_{A-C}	$\sigma_{d_{A-C}}$
Calibrated	728.294	0.003	727.703	0.003	1455.996	0.003
Individual systems						
LT	728.281	0.029	727.653	0.032	1455.930	0.030
PS	728.330	0.089	727.65	0.12	1455.98	0.11
Competitive						
LT + PS	728.257	0.019	727.649	0.019	1455.906	0.016
Cooperative						
LT + PS	728.260	0.018	727.648	0.018	1455.907	0.015
LT + 2C	728.248	0.019	727.676	0.021	1455.924	0.019
LT + 1C	728.288	0.022	727.609	0.023	1455.896	0.019

LT: Laser tracker
PS: photogrammetric system
1C: central camera of the photogrammetric system
2C: two lateral cameras of the photogrammetric system

Table 2 suggests few considerations: (i) the cooperative fusion improves the system performance when compared to the results of the single LVM system, and (ii) the sensor configuration LT + PS drives to the same result, both when implementing the cooperative and the competitive data fusion, however, differently from the competitive approach, the cooperative one can be also profitably applied for the LT + 2C and LT + 1C configurations.

6. Conclusions

This paper presents a structured comparison between the classical competitive approach and a new cooperative approach for fusing data obtained from different LVM systems. The latter approach uses angular and/or distance data, measured by the sensors equipping each LVM system, so as to compute the 3D position of the points of interest. Input data of this model are (i) local measurements (i.e. data concerning their position/orientation) performed by the individual sensors (and relevant uncertainties), and (ii) calibration parameters of the individual sensors.

The main advantages of the proposed approach, with respect to the competitive one, are: (i) it is the only option when the individual LVM systems are not able to provide autonomous position measurements (e.g., laser interferometers or single cameras), (ii) it is the only option when only some of the sensors of autonomous systems work correctly (for instance, a laser tracker in which only distance – not angular – measurements are performed), (iii) when using systems with redundant sensors (i.e. photogrammetric systems with a large number of distributed cameras), point localization tends to be better than that using the competitive fusion approach.

The same considerations do not seem to hold when fusing data from LTs. In this particular case, the difference in performance between cooperative and competitive fusion is not statistically significant.

A limitation of the proposed approach is that it can be applied only to sensors performing angular and distance measurements, with respect to the point of interest.

Future research is aimed at enriching the proposed method so as to take account of the uncertainties related to the sensor localization/orientation parameters that derive from the relative calibration process.

References

API Automated Precision INC. (2015). "Radian TM." Retrieved January 13th, 2015, from http://www.apisensor.com/index.php/products-en/laser-trackers-and-accessories-en/radian-en.

Beckerman, M. and Sweeney, F. J. (1994). "Segmentation and cooperative fusion of laser radar image data." Proceedings of SPIE - The International Society for Optical Engineering **2233**: 88-98.

BIPM, I., IFCC, I., IUPAC, I. and ISO, O. (2008). Evaluation of measurement data—guide for the expression of uncertainty in measurement. JCGM 100: 2008.

Boudjemaa, R. and Forbes, A. B. (2004). "Parameter Estimation Methods for Data Fusion." NPL Report CMSC 38/04.

Budzan, S. (2014). Fusion of visual and range images for object extraction. Lecture Notes in Computer Science (including subseries Lecture Notes in Artificial Intelligence and Lecture Notes in Bioinformatics). **8671:** 108-115.

Caja, J., Gómez, E. and Maresca, P. (2015). "Optical measuring equipments. Part I: Calibration model and uncertainty estimation." Precision Engineering **40**: 298-304.

Calkins, J. M. and Salerno, R. J. (2000). A practical method for evaluating measurement system uncertainty. Boeing Large Scale Metrology Conference, Long Beach, CA.

Crowley, J. L. and Demazeau, Y. (1993). "Principles and techniques for sensor data fusion." Signal Processing **32**(1-2): 5-27.

Durrant-Whyte, H. F. (1988). "Sensor models and multisensor integration." International Journal of Robotics Research **7**(6): 97-113.

Franceschini, F., Galetto, M., Maisano, D., Mastrogiacomo, L. and Pralio, B. (2011). Distributed large-scale dimensional metrology, Springer-Verlag London.

Galetto, M. and Mastrogiacomo, L. (2013). "Corrective algorithms for measurement improvement in MScMS-II (mobile spatial coordinate measurement system)." Precision Engineering **37**(1): 228-234.

Galetto, M., Mastrogiacomo, L., Maisano, D. and Franceschini, F. (2015). "Cooperative fusion of distributed multi-sensor LVM (Large Volume Metrology) systems." CIRP Annals - Manufacturing Technology **64**(1): 483-486.

Haghighat, M. B. A., Aghagolzadeh, A. and Seyedarabi, H. (2011). "Multi-focus image fusion for visual sensor networks in DCT domain." Computers and Electrical Engineering **37**(5): 789-797.

Ho, A. Y. K. and Pong, T. C. (1996). "Cooperative fusion of stereo and motion." Pattern Recognition **29**(1): 121-130.

Kariya, T. and Kurata, H. (2004). Generalized least squares, John Wiley & Sons, Ltd, Chichester, UK.

Labayrade, R., Royere, C., Gruyer, D. and Aubert, D. (2005). "Cooperative fusion for multi-obstacles detection with use of stereovision and laser scanner." Autonomous Robots **19**(2): 117-140.

Lamallem, A., Valet, L. and Coquin, D. (2009). Local versus global evaluation of a cooperative fusion system for 3D image interpretation. ISOT 2009 - International Symposium on Optomechatronic Technologies, Istanbul, IEEE.

Luhmann, T., Robson, S., Kyle, S. and Harley, I., Eds. (2006). Close Range Photogrammetry John Wiley & Sons, New York, NY, USA, .

Maisano, D. and Mastrogiacomo, L. (2015). "A new methodology to design multi-sensor networks for distributed Large-Volume Metrology systems based on triangulation." To appear on Precision Engineering. DOI: 10.1016/j.precisioneng.2015.07.001.

Maisano, D. A., Jamshidi, J., Franceschini, F., Maropoulos, P. G., Mastrogiacomo, L., Mileham, A. R. and Owen, G. W. (2009). "A comparison of two distributed large-volume measurement systems: The mobile spatial co-ordinate measuring system and the indoor global positioning system." Proceedings of the Institution of Mechanical Engineers, Part B: Journal of Engineering Manufacture **223**(5): 511-521.

Mastrogiacomo, L. and Maisano, D. (2010). "Network localization procedures for experimental evaluation of mobile spatial coordinate measuring system (MScMS)." International Journal of Advanced Manufacturing Technology **48**(9-12): 859-870.

NaturalPoint (2015, January 13th). "OptiTrack V120:Trio." from https://www.naturalpoint.com/optitrack/products/v120-trio/.

New River Kinematics (2015). "SpatialAnalyzer®." Retrieved January 13th, 2015, from http://www.kinematics.com/spatialanalyzer/.

Weckenmann, A., Jiang, X., Sommer, K. D., Neuschaefer-Rube, U., Seewig, J., Shaw, L. and Estler, T. (2009). "Multisensor data fusion in dimensional metrology." CIRP Annals - Manufacturing Technology **58**(2): 701-721.

Wen, C. Y., Hsiao, Y. C. and Chan, F. K. (2010). "Cooperative anchor-free position estimation for hierarchical wireless sensor networks." Sensors **10**(2): 1176-1215.

Wolberg, J. (2005). Data Analysis Using the Method of Least Squares: Extracting the Most Information from Experiments, Springer-Verlag Berlin Heidelberg.

Xiong, N. and Svensson, P. (2002). "Multi-sensor management for information fusion: Issues and approaches." Information Fusion **3**(2): 163-186.

Appendix

Table A.1. Mean value, 25th and 75th percentile of the localization error distribution [mm] for the different layouts tested, when combining a LVM system based on triangulation with one based on multilateration. The results obtained by competitive ("Comp.") and cooperative ("Coop.") fusion are reported.

Number of distance sensors

		4			5			6			7			8			9			10		
		Avg.	Q1	Q3	Avg.	Q1	Q3	Avg.	Q1	Q3	Avg.	Q1	Q3	Avg.	Q1	Q3	Avg.	Q1	Q3	Avg.	Q1	Q3
4	Comp.	0.0192	0.0046	0.0217	0.0152	0.0041	0.0178	0.0111	0.0033	0.0126	0.0096	0.0030	0.0116	0.0085	0.0028	0.0102	0.0077	0.0026	0.0091	0.0064	0.0023	0.0074
	Coop.	0.0189	0.0046	0.0216	0.0151	0.0041	0.0178	0.0110	0.0034	0.0125	0.0095	0.0030	0.0115	0.0085	0.0028	0.0102	0.0077	0.0026	0.0090	0.0064	0.0023	0.0075
5	Comp.	0.0189	0.0048	0.0234	0.0129	0.0038	0.0147	0.0106	0.0035	0.0131	0.0095	0.0030	0.0109	0.0088	0.0028	0.0106	0.0073	0.0025	0.0085	0.0073	0.0025	0.0089
	Coop.	0.0188	0.0048	0.0229	0.0129	0.0038	0.0146	0.0106	0.0036	0.0130	0.0094	0.0030	0.0108	0.0088	0.0028	0.0106	0.0072	0.0025	0.0085	0.0073	0.0025	0.0089
6	Comp.	0.0199	0.0050	0.0238	0.0141	0.0040	0.0167	0.0121	0.0035	0.0143	0.0096	0.0030	0.0114	0.0086	0.0028	0.0104	0.0075	0.0026	0.0088	0.0069	0.0024	0.0082
	Coop.	0.0197	0.0050	0.0236	0.0140	0.0039	0.0167	0.0120	0.0035	0.0143	0.0096	0.0030	0.0115	0.0085	0.0028	0.0103	0.0075	0.0026	0.0090	0.0069	0.0024	0.0081
7	Comp.	0.0209	0.0051	0.0251	0.0139	0.0040	0.0167	0.0119	0.0035	0.0138	0.0097	0.0031	0.0118	0.0084	0.0028	0.0100	0.0073	0.0025	0.0086	0.0067	0.0024	0.0080
	Coop.	0.0205	0.0050	0.0247	0.0137	0.0040	0.0166	0.0118	0.0035	0.0138	0.0096	0.0031	0.0118	0.0084	0.0028	0.0099	0.0073	0.0025	0.0085	0.0066	0.0024	0.0079
8	Comp.	0.0186	0.0048	0.0226	0.0136	0.0040	0.0166	0.0123	0.0036	0.0150	0.0095	0.0031	0.0115	0.0082	0.0027	0.0096	0.0075	0.0026	0.0090	0.0069	0.0024	0.0084
	Coop.	0.0183	0.0048	0.0224	0.0136	0.0040	0.0168	0.0123	0.0036	0.0151	0.0095	0.0031	0.0114	0.0081	0.0027	0.0096	0.0075	0.0026	0.0090	0.0069	0.0024	0.0083
9	Comp.	0.0189	0.0051	0.0236	0.0151	0.0043	0.0187	0.0111	0.0034	0.0132	0.0090	0.0029	0.0105	0.0083	0.0028	0.0097	0.0077	0.0026	0.0091	0.0070	0.0024	0.0082
	Coop.	0.0186	0.0050	0.0234	0.0150	0.0043	0.0188	0.0110	0.0034	0.0130	0.0090	0.0029	0.0104	0.0083	0.0028	0.0096	0.0076	0.0026	0.0091	0.0070	0.0024	0.0082
10	Comp.	0.0184	0.0049	0.0221	0.0129	0.0038	0.0150	0.0101	0.0033	0.0119	0.0088	0.0029	0.0103	0.0080	0.0027	0.0095	0.0080	0.0026	0.0093	0.0064	0.0023	0.0077
	Coop.	0.0181	0.0049	0.0221	0.0127	0.0038	0.0150	0.0100	0.0033	0.0118	0.0087	0.0029	0.0102	0.0080	0.0027	0.0096	0.0079	0.0026	0.0092	0.0064	0.0023	0.0077

Number of angular sensors